TECTONICS, VOL. 16, NO. 3, PAGES 409-424, JUNE 1997

Systematic analyses of the large-scale topography and structure across the Dead Sea Rift

Shimon Wdowinski
Department of Geophysics and Planetary Sciences, Tel Aviv University, Ramat Aviv, Israel

Ezra Zilberman
Geological Survey of Israel, Jerusalem

Abstract. The Dead Sea Rift (DSR) is one of the deepest continental depressions on the Earth's surface and is the best example of a continental rift lying along a transform plate boundary (the Dead Sea Transform). We systematically analyze the large-scale topography, structure, and morphology across the central part of the DSR between Lake Kinneret and the Gulf of Elat and show a distinct asymmetrical topographic pattern across the rift axis. The topography analysis uses a Digital Terrain Model (DTM) of Israel and adjacent areas to plot a series of 64 profiles perpendicular to the rift axis. The profiles show that the eastern side is topographically higher than the western side and that its overall shape resembles an uplifted shoulder; the lower western side resembles an arch. This analysis also reveals along-strike variations in the topography that allow us to subdivide the central DSR into five segments of similar topography. The large-scale structure across the DSR is investigated by a series of 10 geological cross sections drawn perpendicular to the rift axis along the five segments. On the basis of the stratigraphic record and the geological history of the region, we identify a regional marker (Top Eocene Sequence) to trace the rift-related structure. This marker shows that the structure parallels the topographic asymmetry across the rift axis: the rift's eastern margin is uplifted toward the axis, whereas the rift's western margin is downflexed toward the axis and defines a wide asymmetrical monocline. Our analyses indicate that (1) the large-scale asymmetry across the DSR reflects a wide half-graben structure (30-60 km wide), (2) the rift's eastern margin reflects broad regional uplift along the rift, and (3) the western side arching is a subsidary structure that follows the main rift structure.

Introduction

The Dead Sea Rift (DSR) is a long and narrow morphological depression extending approximately N-S from the Bakaa Valley (about 150 km north of Lake Kinneret) to the Gulf of Elat (Aqaba) (Figure 1). It is one of the deepest continental depressions on the Earth's surface, with the rift axis lying below sea level for 250 km (half of rift's length). The rift lies along the southern segment of the Dead Sea Transform (DST), which runs from the Zagros Mountains (Turkey) to the Red Sea and separates the Arabian plate from the Israel-Sinai subplate (inset in Figure 1) [*Wilson*, 1965; *Freund et al.*, 1970; *Garfunkel*, 1981].

It is important to emphasize the distinction between the terms Dead Sea Rift (DSR) and Dead Sea Transform (DST), which have been used interchangeably in several studies [e.g., *Garfunkel*, 1981]. Rift is a structural term describing an elongated trough bounded by faults, whereas transform is a plate-tectonic term describing the kinematics between two adjacent plates. Although, in general, tectonic forces acting along plate boundaries give rise to structural and morphologic expressions on the Earth's surface, this is not always the case. A distinct rift exists only along the southern half of the DST plate boundary; the transform's northern half has no marked morphologic expression beside several basins along its northernmost extent.

The large-scale topography and structure across the DSR were examined by several studies but not in a systematic manner. More than a century ago, *Lartet* [1869] drew a geological section across the Dead Sea showing an asymmetrical structure across the rift. Similarly, *Picard* [1960, 1966] drew several geological cross sections showing the asymmetric structural pattern and its variations along the rift's axis. More recently, *ten Brink et al.* [1990] quantitatively described the large-scale topography and gravity anomalies along a single profile across the DSR. However, their profile crosses the rift north of the Dead Sea, where the topography is almost symmetrical and therefore is not representative.

The lack of interest in the large-scale topography and structure across the rift can be attributed to the widely accepted interpretation of the DSR as a transform plate boundary [*Wilson*, 1965; *Freund et al.*, 1970]. Until the theory of plate tectonics was accepted in the late 1960's, the DSR was interpreted as a graben [*Blanckenhorn*, 1893] or a series of half-grabens [*Picard*, 1966] and research focused on vertical movements across the

Paper number 97TC00814.
0278-7407/97/97TC-00814$12.00

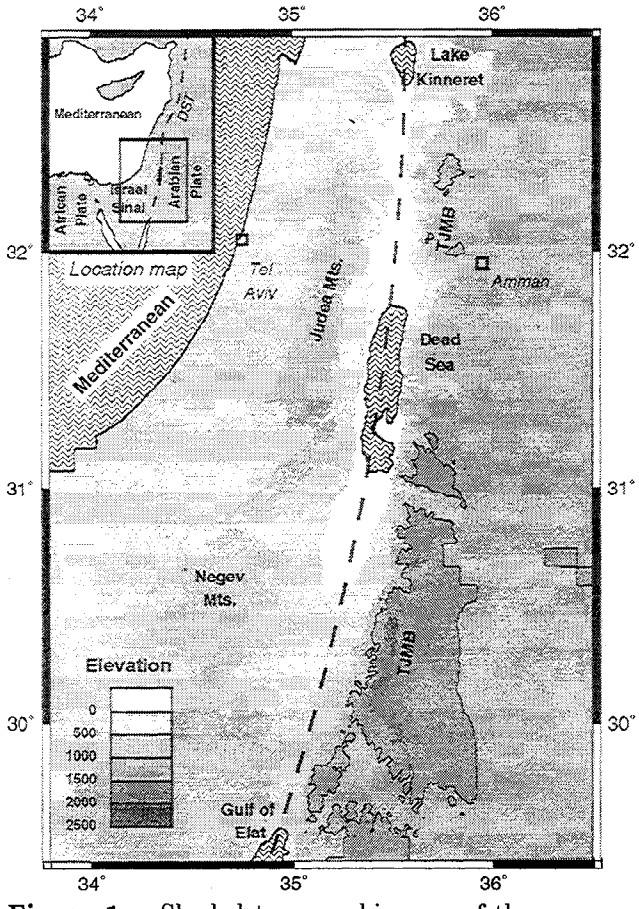

Figure 1. Shaded topographic map of the area surrounding the Dead Sea Rift between Lake Kinneret and the Gulf of Elat. The dashed line shows the location of the small (latitudinal) circle that best describes the rift axis. The thin continuous line around the Trans Jordan Mountain Belt (TJMB) highlands marks the 1000 m elevation contour to emphasize the asymmetric topography across the Dead Sea Rift (DSR). Most of the 1x1 km^2 average elevations were provided by *Hall*'s [1993] Digital Terrain Model (DTM) of Israel. The elevation of areas without DTM coverage were taken from ETOPO-5 [*National Geophysical Data Center (NGDC)*, 1988].

rift. Since the DSR has been recognized as a transform plate boundary, however, most of the tectonic research has focused on structures within the rift valley [e.g., *Garfunkel*, 1981; *Ben Avraham and ten Brink*, 1989; *ten Brink et al.*, 1993] and ignored the larger-scale picture that extends well beyond the rift valley. To our knowledge, the one exception is the study of *ten Brink et al.* [1990], who used topography and gravity anomalies across the rift to investigate isostatic uplift of the rift margins.

This study aims to fill a research gap of 3 decades, during which the large-scale features across the DSR were largely ignored. We systematically analyze the large-scale topography and structure across the central part of the DSR between Lake Kinneret and the Gulf of Elat. We also describe the regional morphology, paleomorphology, geological history, and crustal structure across the DSR, adding important observations about the rift's structure and its evolution with time. Our analyses indicate that the asymmetric large-scale topography and structure across the central segment of the DSR reflects a wide half-graben (40-60 km wide) and a regional uplift along the rift margins. This implies that the large-scale structure and morphology across the DSR cannot be explained solely by horizontal motion along the DST. On the basis of this study's results, *Wdowinski and Zilberman* [1996] present a new isostatically supported half-graben model for the formation of the DSR.

Geologic and Tectonic Background

The geology of the DSR region reflects a history of events that can be divided into three major stages [*Garfunkel*, 1978]: (1) the Precambrian Pan-African orogenic stage, a period of igneous and metamorphic activity that formed the Arabo-Nubian crystalline basement; (2) the Early Cambrian to middle Cenozoic platformal stage, a period of tectonic quiescence, in which an extensive sedimentary sequence was deposited on a stable platform (appendix); and (3) the mid-Cenozoic to recent rifting and continental breakup stage, a period of extensive tectonic activity that broke up the stable platform and formed the present-day topography, structure, and morphology.

The DSR is one of the most pronounced expressions of a continental breakup process that influenced the region since the mid-Cenozoic. The present-day morphology of the DSR was formed in early Pliocene (5-4 Ma) (*Picard*, 1951; *Bentor and Vroman*, 1960) along the trace of the DST. The left-lateral motion along the DST was initiated much earlier, in the early Miocene (23.5 Ma), and has accumulated a total of 105 km [*Fruend et al.*, 1970; *Garfunkel*, 1981]. The displacement along the DST since the formation of the rift in the Pliocene is 30 km [*Joffe and Garfunkel*, 1987].

Most of the exposed rocks along the DSR are sedimentary rocks that were deposited in the region since the Cambrian. The stratigraphic sequence of the exposed and subsurface sedimentary rock column can be roughly subdivided into three major units [*Ball and Ball*, 1953]. The first two units were deposited during the stable platformal stage, whereas the third unit was deposited during continental breakup. The units are (1) lower clastic unit, consisting mainly of continental sandstones, which were deposited since the Cambrian until the end of the Early Cretaceous; (2) middle shallow marine carbonate platform unit, deposited during the Cenomanian to late Eocene regional transgression; and (3) upper clastic unit, consisting of continental sediments, deposited since the early Miocene.

Topography

The large-scale topography across the DSR is quantitatively characterized using a Digital Terrain Model (DTM) of Israel and adjacent areas [*Hall*, 1993]. We use a condensed version of Hall's DTM, in which each square kilometer is represented by a single average elevation (instead of 25x25 m^2 in the full DTM). For regions that are not covered by the DTM, the elevation was obtained from the topographic data set ETOPO-5 [*National Geophysical Data Center*, 1988]. Elevation differences between the two data sets may cause artificial elevation offsets; however, these offsets are smaller than the resolution of the ETOPO-5 and are limited to marginal areas far from the rift axis. Thus the combined topographic data set, as shown in Figure 1, provides a sufficient resolution for a systematic analysis of the large-scale topography. We chose to restrict our analysis to the central part of the DSR between Lake Kinneret and the Gulf of Elat, because along this section of the rift the morphology is well defined and because the DTM data set covers a wide enough area on both sides of the rift. The northern part of the rift (from Lake Kinneret to the Bakaa Valley) is morphologically less pronounced and, furthermore, is only partly covered by the DTM. The southern part of the rift (Gulf of Elat) is not covered at all by the DTM.

The topography of the central DSR is characterized by a long and narrow morphological depression that lies mostly below sea level (Figure 1). In order to characterize the topography across the rift, we define a reference line, the rift axis. The axis, which is located in the center of the morphological depression, can be traced, to a first order, by a small (latitudinal) circle that connects Lake Kinneret, the Dead Sea, and the Gulf of Elat (dashed line in Figure 1). We describe this circle in terms of its Eulerian pole (32.3°N, 22.8°E) and the point (31.5°N, 35.45°E) that lies on the circle. This circle is very similar to the small circle that describes the instantaneous motion along the DST (Eulerian pole (32.8°N, 22.6°E) ± 0.5° and the point (31.5°N, 35.5°E) on the small circle) [*Joffe and Garfunkel*, 1987].

The topography across the rift is analyzed using a series of 64 profiles perpendicular to the rift axis that are spaced 5-6 km from one another (Figure 2). The profiles are divided into five groups that show a similar topographic pattern (up to 400 m deviation from a mean topographic curve) on both sides of the rift (Figure 3). Each group of profiles represents a 40-80 km wide segment perpendicular to the rift axis (Figure 2). The division into groups of similar topography was conducted independently for each side of the rift but was found to be very similar with respect to the width and location of each group on both sides of the rift. Twelve profiles were not included in any of the groups because they represent transitional topography between groups (profiles 1-3, 13, 28, 40, 41, 50-52, 63, and 64).

All the profiles show a narrow rift morphology (10-20 km wide) that lies below or slightly above sea level and an asymmetrical topographic pattern across the rift. East of the rift axis, the topography rises sharply by 1400-1700 m to the peaks of Transjordan Mountain Belt (TJMB in Figure 1), which lie 20-30 km away. From this high elevation (1000-1500 m above sea level), the topography decreases gradually to a desert plateau at an elevation of 700-900 m, within 30-50 km. The overall shape of the rift's eastern margin topography resembles an uplifted shoulder. West of the rift, the topography rises from the rift axis by 1000-1500 m to the peaks of the Judean and Negev Mountains within a distance of 30-60 km (Figure 1). From the peaks of the mountains, the topography decreases to the Mediterranean or to the Negev and Sinai lowlands. The overall topography of the rift's western margin resembles a gentle asymmetrical arch.

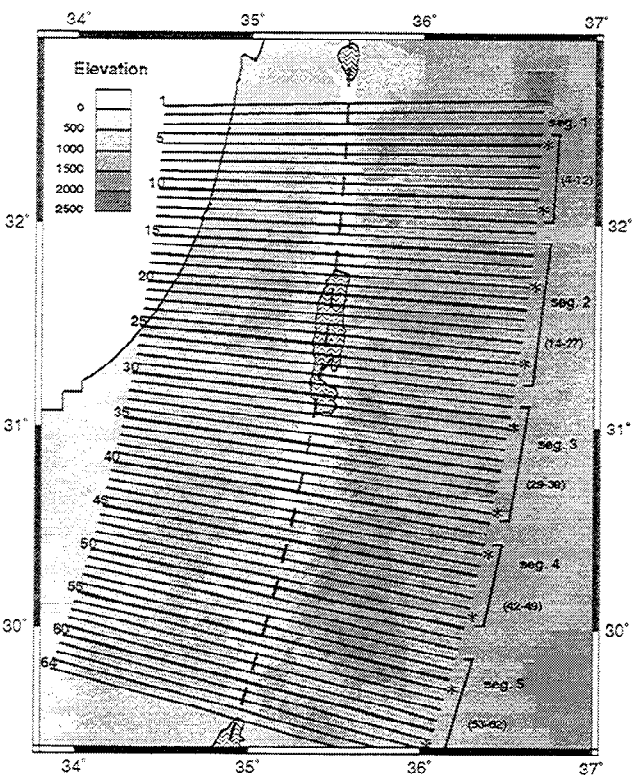

Figure 2. Location map of 64 topographic and the 10 structural sections across the DSR. The sections are drawn perpendicular to the plate boundary, which is represented by the small circle (dashed line), and are spaced 5-6 km apart. The sections marked by an asterisk indicate the location of the 10 geological cross sections shown in Figure 6. The map also displays the locations of the five segments that show similar long wavelength topography (see text and Figure 3).

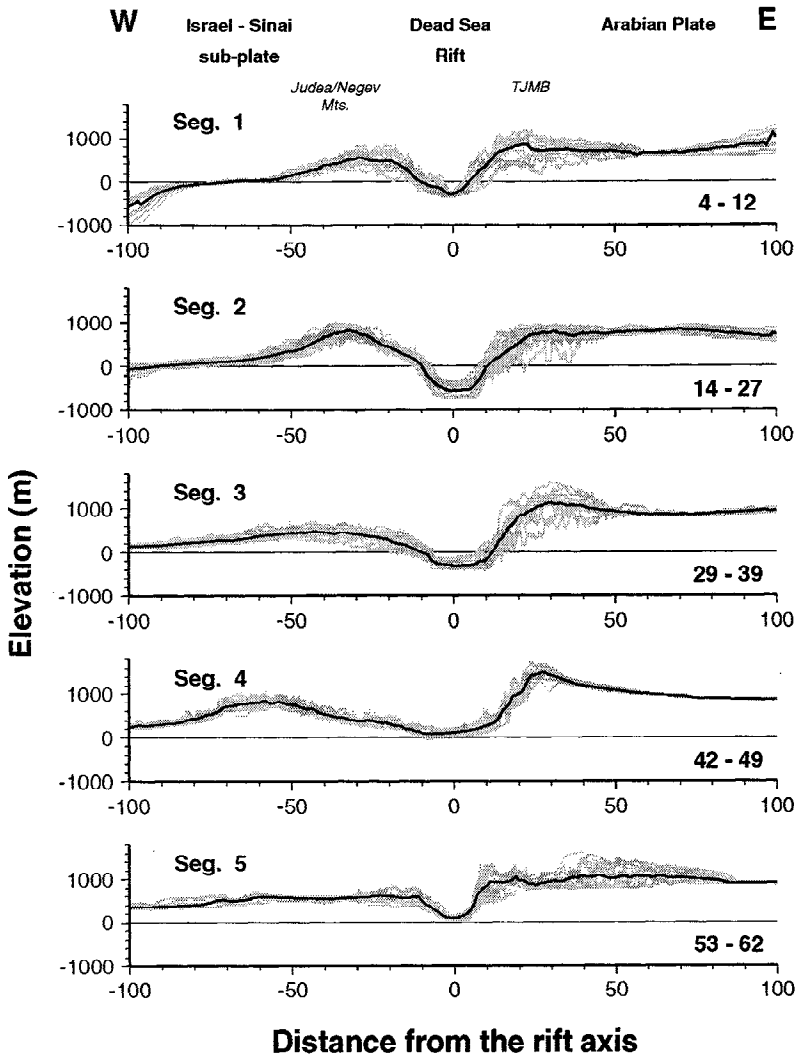

Figure 3. Topographic profiles across the DSR (location in Figure 2). The profiles are divided into five groups of similar long-wavelength topography. Within each segment, individual profiles are shown in gray, and the average topography profile is black. All sections show the narrow rift morphology (10-20 km wide) and the much wider region of elevated topography (100-200 km wide). Each profile contains 1500-1800 data points separated by 100 m, provided mostly from *Hall*'s [1993] DTM of Israel. Data points that lie beyond the DTM coverage were taken from ETOPO-5 [*NGDC*, 1988].

The asymmetry across the DSR, that is an uplifted shoulder in the east and asymmetric arch in the west, is evident along most of the studied region. However, this description is only partly valid in segments 2 and 5, although the sense of asymmetry is still preserved in both of the segments. Segment 2 lacks the eastern side's uplifted shoulder, but the shape of the two sides are very different from one another. Segment 5 lacks the western side's arching, but the eastern side is still higher than the western side.

The topographic asymmetry can be quantified by plotting the highest elevations along the western and the eastern margins. This is done in Figure 4a, which shows that along most of the rift's length, the eastern side is higher than the western side. Only along a short portion of segment 2, which lies along the northern basin of the Dead Sea, the western side is higher than the eastern side. Another unique characteristic of segment 2 is the flat shape of the eastern shoulder, which differs markedly from the other segments (Figure 3). It is interesting to note that the curve describing the elevation of the highest points on the western side is more of a mirror image to the curve describing the elevation of the rift axis (Figure 4a). In other words, the highest part on the western side (max-W in Figure 4a) lies along the lowest part of the rift axis (min-R), and vice versa, the lowest part of the western side lies along the highest part of the rift axis. On the other hand,

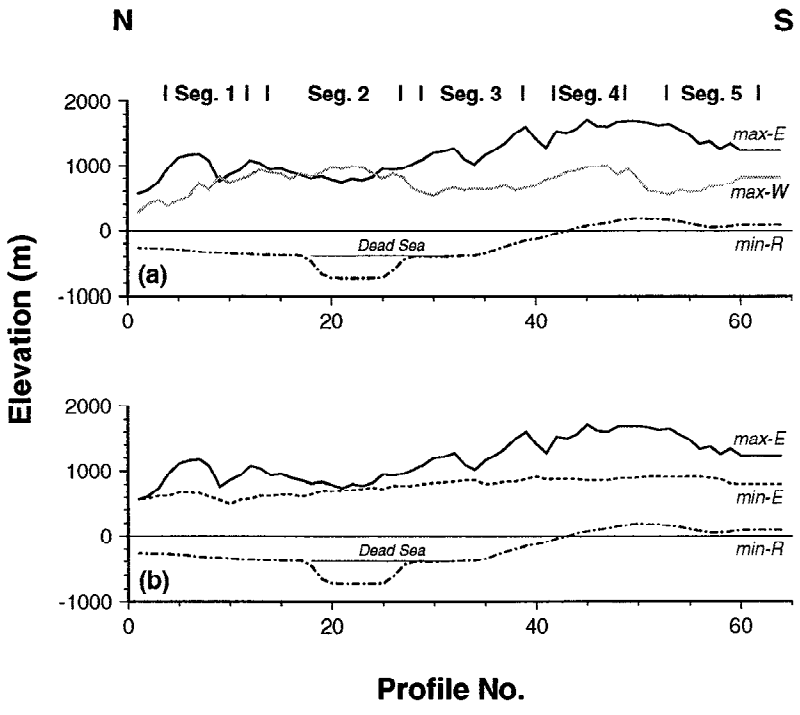

Figure 4. Topographic sections parallel to the rift axis. (a) Profiles along the rift axis (min-R, dotted-dashed line) and along the highest points of both margins: the western (max-W, gray line) and the eastern (max-E, black line). (b) Profiles along rift axis (min-R), the highest points in the eastern margin (max-E), and the lowest point east of the margin in the Transjordan desert plateau (min-E, dashed line). Each of the three curves contains 64 elevation points, which were derived from the 64 topographic profiles (x axis) and as a result has a ragged shape.

the curve describing the elevation of the highest points on the eastern side (max-E) resembles to a first degree that of the rift axis. This indicates an almost constant elevation difference (1500-1700 m) between the uplifted eastern margin and the rift axis along most of the rift's length. However, while the topography is higher in the east, the height of the shoulder above the base level is lower in the east (0-600 m) than in the west (500-1000 m).

Structure

The regional structural pattern comprises three major structural systems (Figure 5). The DSR is the youngest and the most pronounced system. The two older systems are the Syrian Arc Fold Belt (SAFB) and the Sinai-Negev Shear Zone (SNSZ) [*Bentor and Vroman*, 1954; *Bartov*, 1974]. The SAFB comprises asymmetric cylindrical folds, which form a huge S-shaped belt extending from central Sinai to Syria. Its central part is parallel to the DSR, whereas its southern and northern segments deviate from the N-S trend to a NE-SW direction. The individual folds are characterized by a width of 5-30 km and amplitude of 0.2-1.5 km. The SNSZ comprises six E-W oriented faults showing dextral displacement of up to 3.5 km [*Bartov*, 1974].

The SAFB and SNSZ started to develop in the early Senonian (85 Ma) [*Bentor and Vroman*, 1951, 1954, 1960; *Bartov*, 1974]. They formed and evolved under a regional WNW-ESE compressional stress field (the Syrian Arc Stress field (SAS)) that dominated the region from the Turonian to the Miocene [*Eyal and Reches*, 1983; *Eyal and Negev*, 1991; *Eyal*, 1996]. During the Miocene, contemporaneous with the formation of the DST, the regional stress field changed to an ENE-WSW extensional field (the Dead Sea Stress field (DSS)) [*Eyal and Reches*, 1983]. However, many geological observations indicate that the SAS continued to influence the region from middle Miocene up to the Recent, as a regional weak stress field [*Eyal and Negev*, 1991; *Eyal*, 1996].

The structures associated with the formation of the DSR are difficult to describe, because west of the rift they are superimposed on prerift structures (e.g., SAFB). In order to trace the rift-related structures, we identify a regional stratigraphic marker, the Top Eocene Sequence (TES). The Eocene sequence was deposited during the last regional transgression, which was the most prominent in the eastern Mediterranean region, covering an area over 1000 km south of the present-day coast [*Garfunkel*, 1978]. More than 100 m of eustatic sea level rise in the Eocene [*Haq et al.*, 1987] and local subsidence

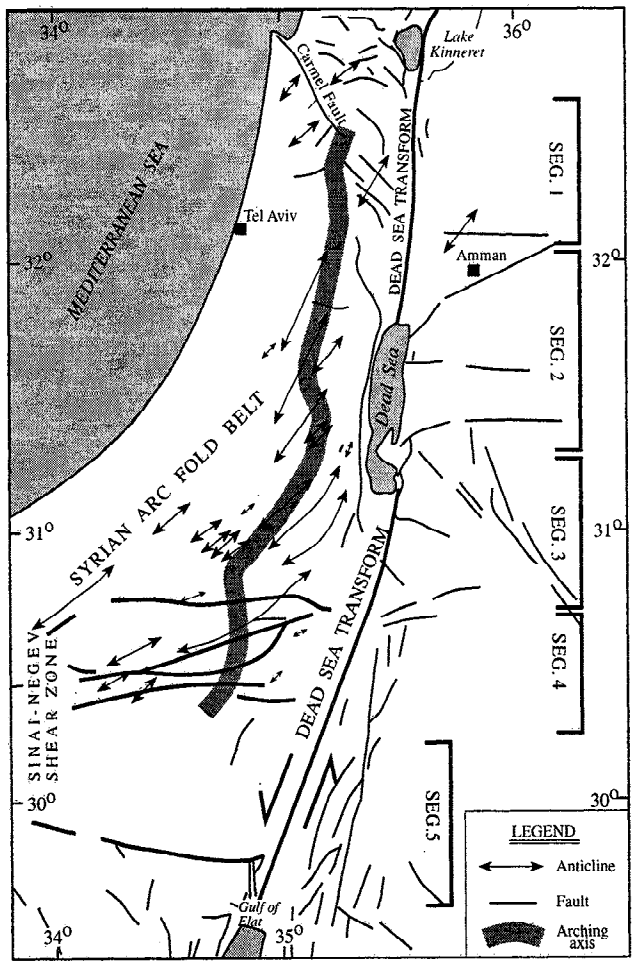

Figure 5. Map of the structural elements in studied area [after *Bartov*, 1990] and their relation to the topographic segmentation (Figure 2). The map shows the location of the major faults along the DSR, the arching axis, and the folds and faults of the two older structural systems: the Syrian Arc Fold Belt and the Sinai Negev Shear Zone. The elongated brackets along the figure's right hand side show the location of the five segemnets.

resulted in the accumulation of a thick sedimentary sequence reaching up to 600 m thickness in the coastal plain of Israel [*Gvirtzman*, 1970] and up to 300 m in the synclines of the SAFB [*Bentor and Vroman*, 1951]. Outcrops of Eocene sediments are found on both sides of the rift but were eroded from most of the anticlines of the SAFB and from the summits of the Transjordan Mountain Belt. However, scattered outcrops of Eocene sediments are found on top of a few high structures of the SAFB in the Negev [*Bentor and Vroman*, 1964; *Avni*, 1989] and at the northern edge of the Judean anticlinorium [*Mimran*, 1984]. These observations indicate that the Eocene sequence covered the previous relief of the SAFB forming a flat sedimentary surface. The final regression at the end of the Eocene exposed a flat sea bottom, which was subjected to limited erosion and remained almost undeformed during the Oligocene (38-23.5 Ma) [*Picard*, 1943; *Garfunkel and Horowitz*, 1966; *Zilberman*, 1992] (for further details see the section on morphology and paleomorphology). The preservation of the post-Eocene low relief morphology throughout the Oligocene indicates a tectonically quiet period in the region [*Garfunkel and Horowitz*, 1966; *Zilberman*, 1992].

On the basis of the above geological history, we adopt the following working hypotheses: (1) Eocene rocks were deposited in the entire region (forming at least a 100 m thick rock column) and covered the previous relief. (2) The top of the Eocene sequence (TES) formed a continuous flat surface slightly inclined toward the open Tethys Sea in the northwest. (3) During the Oligocene, the TES experienced negligible deformation. (4) Upward or downward deflection of the TES represents the total vertical displacement since the early Miocene (23.5 Ma) to the present. These assumptions provide us with a useful tool, albeit with a crude resolution (200-300 m), to detect the rift-related structure.

Figure 6 shows 10 geological sections, (two representative sections per segment) that trace and reconstruct the TES across the DSR. The sections are based on the 1:750,000 geological photomap of Israel and adjacent areas [*Bartov*, 1990], which provide sufficient resolution to detect the long wavelength structure across the rift. We used seven major rock units, mostly sedimentary (Table 1), to present the large-scale structure across the rift. A more detailed description of the main rock units is presented in the appendix. The thickness of the units west of the rift (Israel) are taken mainly from *Freund et al.* [1970] and *Bartov et al.* [1972] but also from many other studies. The thickness of the units east of the rift (Jordan) are taken from *Bender* [1968, 1974], *Freund et al.* [1970], and *Powell* [1989]. Additional information about the thickness of rock units east of the rift was extrapolated from the western side after correcting for the 105 km left-lateral displacement along the DST.

In places where the TES is eroded, we traced its vertical location by estimating the thickness of the missing sedimentary rock column (Table 1). The reconstruction of the TES in the coastal plane and in the Transjordan plateau is straightforward because (1) some of the Eocene sediments are still in site and (2) thickness variations within the Eocene sequence and within the rock unit underneath are very gradual. The reconstruction of the TES across the SAFB structures requires the consideration of thickness variations within the Eocene sequence and the rock unit underneath (Mount Scopus Group) between synclines and anticlines. In general, both units are thicker by 200-400 m in the synclines than in the anticlines. Owing to the intensive erosion of the entire sedimentary cover in the southern part of the Transjordan plateau, the resolution of the TES in segment 5 is worse than the other northern segments.

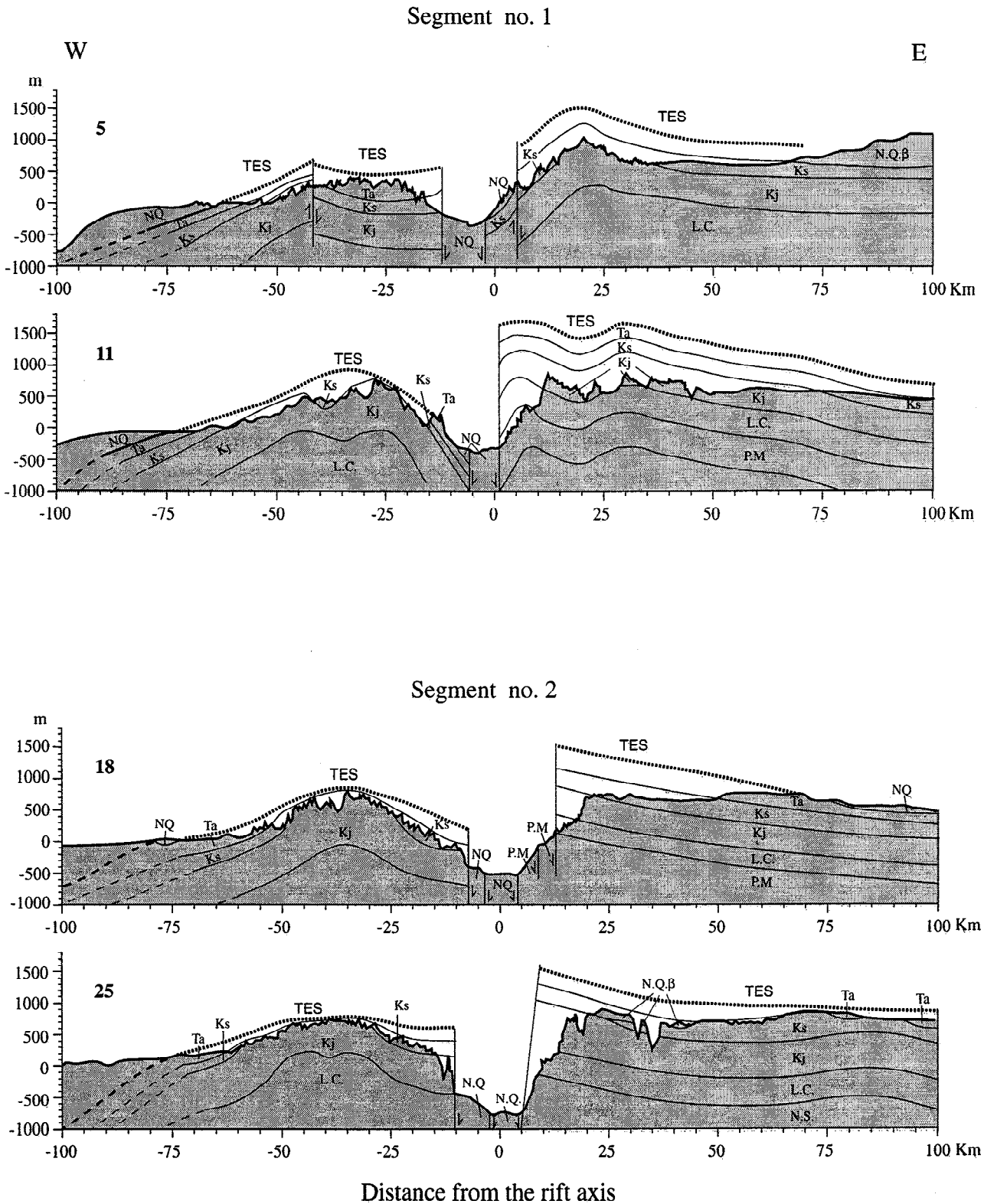

Figure 6. Representative geologic sections (two per segment) across the DSR. The sections show the major rock units, large-scale structure, and the reconstructed location of the TES marker perpendicular to the rift axis. The rock units are described in Table 1.

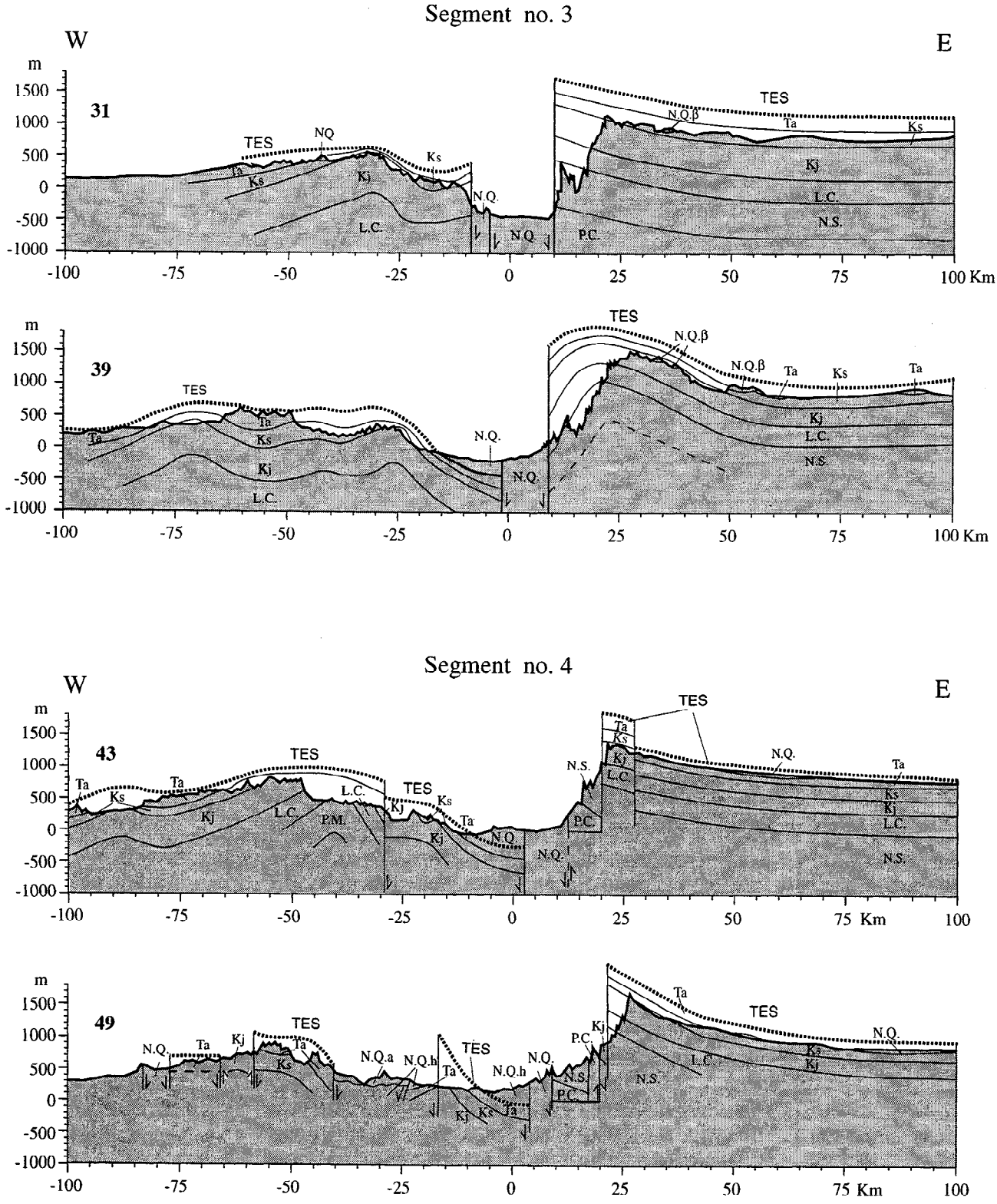

Figure 6. (continued)

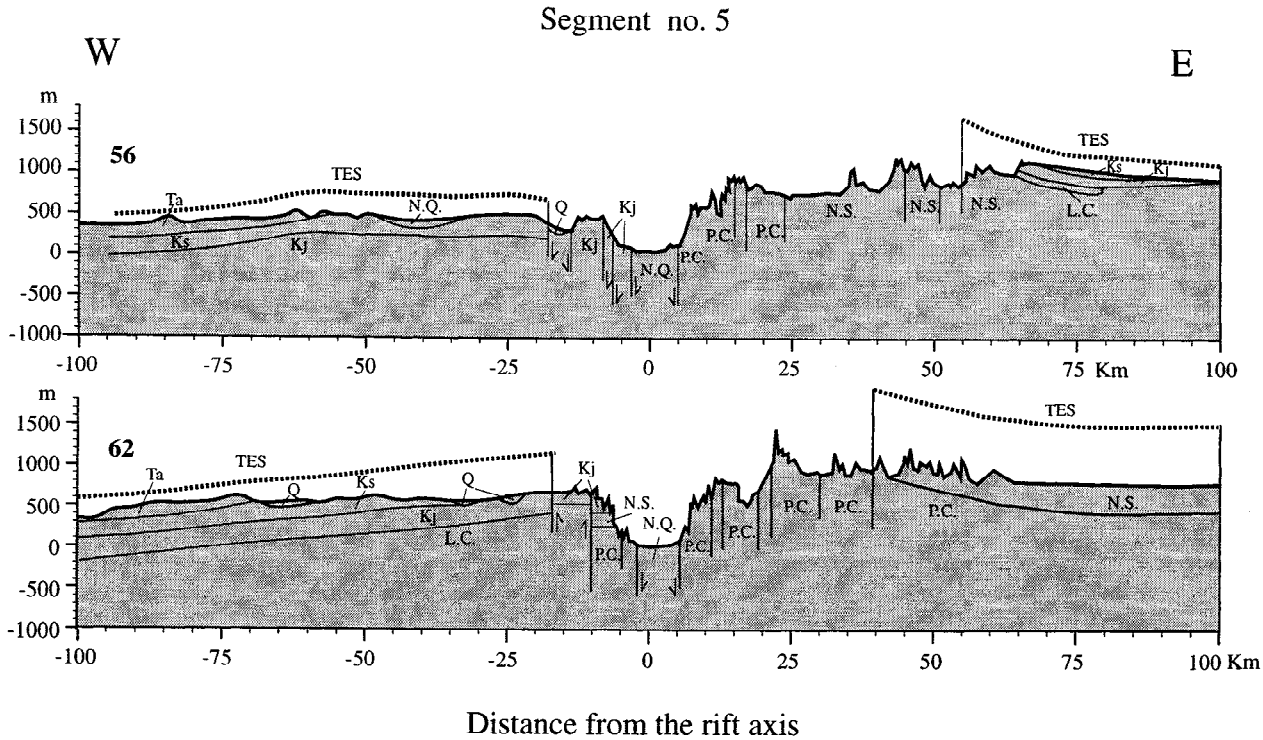

Figure 6. (continued)

The large-scale structure across the DSR also shows an asymmetrical pattern (Figure 6), similar to that of the topography. The structure east of the rift axis is characterized by an upward flexure of the rift margin, whereas the structure west of the axis is characterized by a downward flexure of the margin toward the rift axis. The overall shape of the western side structure (segments 1-4) resembles an asymmetric anticline,

Table 1. Major Rock Unit Used in the Geological Cross Sections and Regional Marker, the Top Eocene Sequence

Symbol	Age	Rock Unit	Thickness
NQ	Neogene-Quarter (Miocene-Pleistocene)	Dead Sea Group, Hazeva Formation	0-6000
	Top Eocene Sequence		
T_a	Tertiary (Eocene)	Avedat Group	100-600
K_s	Cretaceous - Early Tertiary (Senonian-Paleocene)	Mount Scopus Group, Belqa Group	0-450
K_j	Cretaceous (Cenomanian-Turonian)	Judea Group, Ajlun Group	160-1000
LC	Cretaceous (Lower)	Kurnub Group	130-450
PM	Late Paleozoic - Early Mesozoic (Permian-Jurassic)	Negev Group, Ramon Group, Arad Group, Main Formation	0-2000
NS	Paleozoic (Cambrian-Silurian)	Yam Suf Group, Ram Group	300-700
PC	Precambrian (basement)		

Units are after *Bartov* [1990]; See appendix for thickness; See text for discussion of the Top Eocene Sequence

which *Picard* [1943] named arching. The width of the arching lies in the range of 60-100 km. The transition between the two structures lies within the narrow depression of the rift, which is filled by a thick sequence (up to 10 km) of continental sediments.

As discussed above, vertical movements associated with the formation of the rift can be detected by the TES marker. This marker follows the overall asymmetrical structure of the rift's uplifted eastern margin and the long wavelength arching west of the rift. However, the structure described by the TES is smoother and of lower amplitude than the overall structure that is described by other units, for example the Judea and Ajlun groups (K_j). This difference in amplitude and smoothness is attributed to the variable thickness of the Mount Scopus and Belqa groups (K_s) and the Avdat group (T_a). (Table 1) over the existing structural relief. However, some of the smoothness of the TES can be attributed to our reconstruction, which has an accuracy of the order of 200-300 m. Nonetheless, the large-scale structure represented by the TES marker shows elevation differences of the order of 500-2500 m, which provide a sufficient level of confidence to use this marker.

The upward deflection of the TES in the eastern side is observed in all 10 sections. However, in three sections (5 and 11 in segment 1 and 39 in segment 3) the westernmost part is tilted toward the rift, showing a smaller-scale fold structure east of the rift. The upward deflection lies in the range of 400-800 m, which occurs over a horizontal distance of 60-80 km. The downward deflection of the western side in the first four segments forms an arch-shaped surface with an amplitude of 500-1200 m and width of 60-100 km. Only segment 5 displays a different pattern, showing upward deflection of both rift margins, which is characteristic of the structure farther south along the Gulf of Elat. Structural variations along the rift axis can be seen in the 10 geological sections of Figure 6. However, we cannot quantitatively subdivide them into segments of similar structure, as in the topography analysis, because a structural data set with the same resolution as the DTM does not exist.

Morphology and Paleomorphology

The regional morphology and its changes through time are the best observations to indicate the temporal evolution of the development of the DSR. The present-day morphology of the area reflects mainly the tectonic activity and surface processes that postdated the regression of the Tethys Sea at the end of the Eocene. The evolution of the morphology from the Eocene to the present has been studied by analyses of drainage systems, regional denudational surfaces, and relicts of continental sediments [*Picard*, 1951; *Quennell*, 1958; *Garfunkel and Horowitz*, 1966; *Zilberman*, 1984, 1990].

The main morphological elements follow a general N-S direction parallel to the DSR. The list of elements from west to east is as follows: the coastal plain, the central mountain belt (Judea and Negev Mountains), the inland deep basin (DSR and the Gulf of Elat), the Transjordan Mountains, and the Transjordan Plateau (Figure 7). The large-scale morphological structure is well expressed by the configuration of the regional drainage networks. There are three drainage systems separated by two water divides, one west of the rift along the central mountain belt and the other east of the rift along the eastern rift margin. The three drainage systems are the Mediterranean, the DSR, and the Transjordan closed drainage basins (Figure 7). The DSR drainage system has two base levels, the Dead Sea (-400 m) and the Gulf of Elat (sea level), which are separated in the central Arava Valley at an elevation of 200 m. The Transjordan closed drainage basins (El Azaraq in the north and El Jafar in the south) lie at an elevation of 700-900 m above sea level.

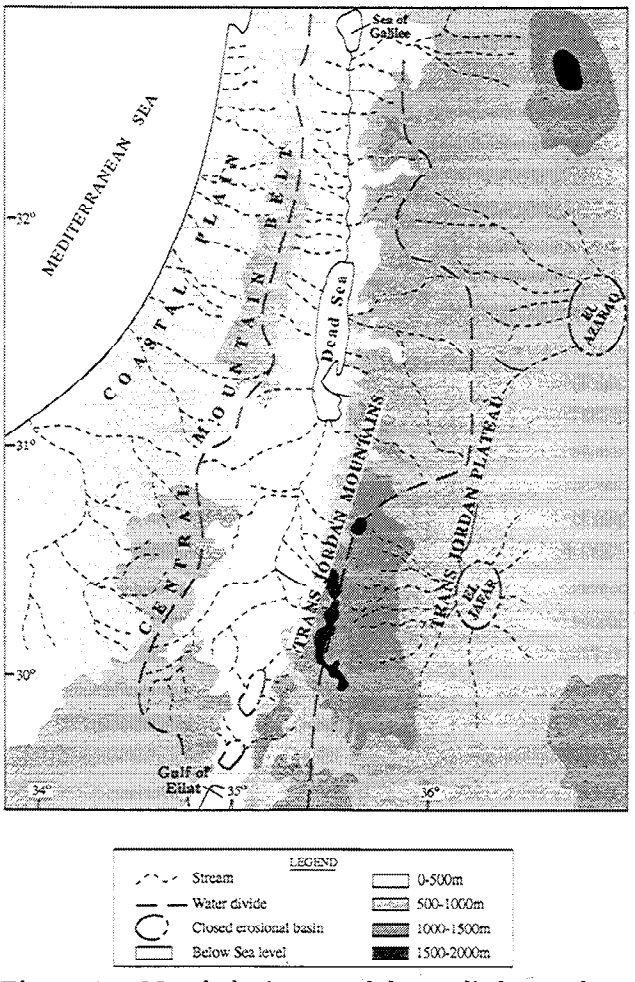

Figure 7. Morphologic map of the studied area showing the topography (gray scale), main morphological elements (boldface), the water divide (long-dashed lines), and the drainage networks (short-dashed lines).

Remnants of a regional low-relief landscape (peneplain), which formed during the Oligocene, are widespread on both sides of the rift [*Picard*, 1951; *Quennell*, 1958, 1984; *Garfunkel and Horowitz*, 1966; *Zilberman*, 1984, 1990]. These remnants include the Transjordan Plateau, the central Negev and Sinai highlands, and the flat erosional surface that truncates the Judea Mountains. Throughout the Negev, the remnants of the low-relief landscape are covered by Miocene fluvial sediments deposited by a regional, northwest flowing drainage system, which originated east of the rift [*Picard*, 1951; *Bentor and Vroman*, 1951, 1960; *Garfunkel and Horowitz*, 1966; *Zilberman*, 1984, 1990]. These fluvial sediments were also found on the eastern margins of the DSR [*Bender*, 1968; *Wetzel and Morton*, 1959; *Steinitz and Bartov*, 1991]. The lateral extent of the Oligocene peneplain and the overlying Miocene fluvial sediments on both sides of the DSR indicate that during the Oligocene and the Miocene both sides of the rift were part of a continuous low-relief terrain, which drained northwestward to the Mediterranean [*Picard*, 1951; *Garfunkel and Horowitz*, 1966; *Garfunkel*, 1981, 1988; *Steinitz and Bartov*, 1991; *Zilberman*, 1992].

The break up of the low-relief landscape and the development of the DSR occurred in the early Pliocene (5-4 Ma) [*Garfunkel and Horowitz*, 1966; *Garfunkel*, 1981, 1988; *Zilberman*, 1992]. This major change in the morphology is manifested by the establishment of the DSR drainage system [*Garfunkel and Horowitz*, 1966; *Zilberman*, 1984, 1990] and by the distribution of fluvial-lacustrine Pliocene sediments within the narrow rift valley [*Picard*, 1943, 1951; *Bentor and Vroman*, 1957, 1960]. The development of the DSR along the DST was attributed by *Garfunkel* [1981] to a change in the sense of motion along the DST from parallel to the rift to slightly oblique. He estimated the additional extensional component, perpendicular to the transform plate boundary, as 2-5 km.

Crustal Structure

The deeper structure across the rift has been obtained by gravity and seismic refraction studies. Both types of studies detect depth variations of two markers: the upper surface of the crystalline basement and the Moho. The upper surface of the crystalline basement between the Dead Sea Rift and the Mediterranean Sea is detected at depth of 3-7 km below sea level and shows a wide E-W arch shape [*Ginzburg and Folkman*, 1981; *ten Brink et al.*, 1990, 1993]. The location and shape of this surface coincides with that of the topography and geologically determined arching. East of the rift, the crystalline basement is detected at depth of 0-5 km and shows an eastward inclination toward the Arabian shield [*El-Isa et al.*, 1987; *ten Brink et al.*, 1990, 1993]. Again, the shape of this marker follows the overall trend of the uplifted eastern margin. The Moho is detected at depth of 20-37 km and shows an overall southeastward trend of crustal thickening from the Mediterranean to the Arabian shield [*Ginzburg and Folkman*, 1980; *El-Isa et al.*, 1987; *ten Brink et al.*, 1990]. Although the gravity data do not indicate Moho depth variation beneath the rift [*Kovach and Ben Avraham*, 1985; *ten Brink et al.*, 1993], seismic refraction studies show a small local crustal thinning underneath the DSR [*Ginzburg and Folkman*, 1980; *El-Isa et al.*, 1987].

Discussion

Large-Scale Asymmetries Across the DSR

Our systematic analyses reveal a distinct asymmetrical topographic and structural pattern across the rift axis. The rift's eastern side is topographically and structurally higher and is upwardly flexed toward the rift axis, whereas the lower western side is downflexed toward the axis. This large-scale asymmetry reflects a wide half-graben structure (30-60 km wide), in which the boundary fault lies along the rift's eastern margin (Figure 6). The hanging wall, the rift's western side, is tilted from its hinge along the Judea/Negev mountain belt eastward to the rift axis. The large-scale half-graben structure is truncated by several normal faults, mostly near of the rift, giving the narrow rift valley the shape of a full graben. Smaller-scale folds (up to 20 km wide) characterize both the hanging wall and foot wall. The folds in the western side hanging wall mostly reflect the anticlines of the SAFB. The downflexing folds along the eastern side footwall toward the rift (sections 5, 11, and 39 in Figure 6) probably reflect subsurface normal faulting east of rift's eastern margin. *Wdowinski and Zilberman* [1996] modeled the large-scale structure across the DSR and estimated the dimensions of an assumed elliptical boundary fault as 15 km deep and 35-60 km long.

The observed large-scale asymmetrical structure across the DSR is also detected along the upper surface of the crystalline basement [*Ginzburg and Folkman*, 1981; *El-Isa et al.*, 1987; *ten Brink et al.*, 1990, 1993]. The similar shape and location of the surface and deep structures indicate that the observed long wavelength surface structures (i.e., arching and uplifted shoulder) are part of a large structure existing throughout the upper crust. Therefore the short wavelength near surface SAFB structures have a minor influence on the large and deep structure. At a deeper level, as detected by the deflection of the Moho, only the eastern side structure follows the surface structure. Both sides show a low-magnitude upward deflection of the Moho beneath the rift [*Ginzburg and Folkman*, 1980; *El-Isa et al.*, 1987].

The regional scale asymmetric topography and structure across the DSR are most evident along the central

segment of the rift, between the Gulf of Elat and Lake Kinneret (29.5-33°N) (Figure 1). Farther north, along the Hula Basin and the Bakaa Valley segments (33-34°N, beyond the northern edge of the map in Figure 1), the DSR has a similar asymmetric pattern but with opposite sense of displacement [*Picard*, 1966, 1987]: the topography and structure of the rift's western side is higher than that of the eastern side, but this is not as pronounced as in the central segment. A similar pattern of half-grabens with alternating sense of displacement is well documented in structural studies of the East African Rift [e.g., *Rosendahl*, 1987; *Ebinger et al.*, 1989]. Farther south, along the Gulf of Elat (28°-29.5°N), the asymmetric pattern is less pronounced, mainly because both sides of the rift are uplifted and eroded. However, the topography of the eastern side is still higher than that of the western side.

The well-marked structural asymmetry is characteristic of the regional scale (100-200 km wide) structure across the DSR. Within the narrow rift margins of the DSR, long and narrow structures (<20 km wide) are dominant [*Quennell*, 1959; *Freund et al.*, 1970; *Garfunkel*, 1981]. These structures include pull-apart basins, rhomb-shaped grabens, and push-up structures and are associated with the horizontal motion along the Dead Sea Transform. The scale difference between the two sets of structures suggests an interesting deformation partitioning in this transtensional tectonic environment. The regional scale structure indicates vertical motion along the rift, whereas the narrower scale structures, which are representative of the horizontal motion, can be viewed as superimposed on the larger-scale structure.

Regional Uplift Along the DSR

The topographic analysis shows that the shape of the rift's eastern margin resembles an uplifted shoulder, which is a characteristic feature of many rifts (e.g., the East African Rift), reflecting regional uplift along the rift. Indeed, the structural analysis detects 1000-1500 m uplift of the rift's eastern margin, which decays eastward with distance from the rift. The topography and structure of the rift's western side lack the characteristic features of an uplifted rift margin because it composes the hanging wall of a wide half-graben structure. Regional uplift beneath rifts can be caused by several mechanisms: surface unloading, thermal processes, or mantle upwelling. The low thermal activity along the DSR suggests that the uplift most likely reflects surface unloading due to the extension, or upwelling beneath the rift, which has not yet propogated to the surface by conduction.

Ten Brink et al. [1990] used kinematic elastic plate models to calculate the uplifted topography across a single profile north of the Dead Sea (segment 2). They estimated the uplift as 700-900 m, with half width of 100-125 km, and attributed the uplift to a deep thermal source. *Wdowinski and Zilberman* [1996] used a kinematic isostatically supported half-graben model to calculate the average uplifted structure across the central segment of the DSR (segments 1-4). They estimated the uplift as 1100-1300 m, with a half width of 80-100 km. They attributed the uplift mostly to surface unloading, caused by 3-6 km of horizontal extension perpendicular to the rift and additional load. The results of *Wdowinski and Zilberman* [1996] may overestimate the tectonic uplift, because the structural uplift often amplifies the tectonic uplift due to erosion and isostatic rebound [*Garfunkel*, 1988; *Steckler and Omar*, 1994].

Arching

Our structural analysis indicates that a significant portion of the western side arching has developed since the Miocene. This result confirms *Salamon*'s [1987] structural analysis of several monoclines in the northern Negev, in which he calculated that half of the arching's 400 m amplitude has developed after the early Miocene. However, paleomorphological observations indicate that this phase of uplift occurred mostly in the Pliocene, as suggested by *Picard* [1943]. All of these age estimates indicate that the arching formed contemporaneously with the horizontal motion along the DST and partly contemporaneously with the formation of the rift in the Pliocene.

The formation of the arching illustrates the problematic relations between the regional stress fields and the arching geometry. The N-S strike of the arching (Figure 5) is subparallel to the rift's axis and hence is almost parallel to the maximum compression of the dominant Dead Sea Stress field (DSS). The arching's strike also lies at an angle of 30°-50° to the maximum compression of the weaker Syrian Arc Stress Field. Therefore neither of these stress fields can explain the formation of the arching.

Salamon [1987] attributed the formation of the arching to vertical movements associated with the formation of the DSR, most likely due to an uplift of the rift's margins. He suggested that the arching reflects subsidence of the eastern slope toward the rift and subsidence of the western slope toward the Mediterranean's passive margins. *Wdowinski and Zilberman* [1996] explained the contemporaneous formation of the DSR and the arching using a two-dimensional isostatically supported half-graben model. The model considers the sum relief of three surfaces: relief that existed prior to the formation of the rift (initial topography), relief created by slip along a curved normal boundary fault (kinematic topography), and relief created by isostatic response of the lithosphere to this faulting and to an additional unmodeled load (isostatic topography). The model pro-

vides a mechanical explanation for the arching formation in a primarily extensional environment. According to the model, the western slope of the arching reflects the initially inclined prerift topography, and the eastern slope reflects the downward flexure of the rift's western margin toward the rift axis. The wide isostatic uplift across the rift added to the arching amplitude but did not affect its width.

The kinematic model of *Wdowinski and Zilberman* [1996] also explains the change in the regional drainage system that followed the rift's formation. According to their model the isostatic uplift of the rift's margins and the formation of the arching broke the prerift single regional drainage system into the present-day three drainage systems. The three drainage systems are the Mediterranean, which extends west of the arching, the Transjordan closed drainage basins, which extends east of the rift, and the DSR drainage system that lies along the rift (Figure 3).

Systematic Analyses of Topography and Structure

In recent years, Digital Terrain Models (DTM) have became an important tool in quantitative description of linear topographic features. One approach for characterizing the first order topography across long mountain ranges has been obtained by stacking a series of sparsely spaced parallel profiles [e.g., *Wdowinski and Bock*, 1994]. Another approach for rigorous characterizing of topographic variations across orogenic fronts and rift valleys has been obtained by swath-averaged topographic profiles [*Masek et al.*, 1994a, 1994b]. However, both methods characterize the first-order along-strike topography profile and ignore along-strike variations. In order to account for second-order features, which vary along strike, we combine both methods and use a series of closely spaced profiles along the central segment of the DSR. Our systematic analysis provides: (1) a quantitative characterization of the large-scale asymmetric pattern across the rift, (2) characterization of the along-strike topography variations according to five segments of similar topography, and (3) identification of anomalous topography (segment 2) along the rift. This analysis also emphasizes the importance of a good DTM, or any other good data set, for obtaining useful quantitative results.

Although the DSR lies along a transform plate boundary (the DST), our analyses consider only the present-day configuration and ignore any contribution that may have resulted from the horizontal displacement along the transform. This strategy is reasonable in the topography analysis, because the large-scale topography reflects the present-day force balance between the tectonic and buoyancy forces [*Wdowinski and O'Connell*, 1990]. However, ignoring the horizontal motion is more problematic in the structural analysis, because the present-day structure juxtaposes structures that were formed and evolved at different locations across the rift. This problem is less acute than one may think, because the displacement across the transform since the formation of the rift, in the early Pliocene (5-4 Ma), is only 30 km [*Joffe and Garfunkel*, 1987] and not 105 km, which is the total displacement across the transform since its initiation in the early Miocene [*Freund et al.*, 1970; *Garfunkel*, 1981]. Furthermore, our analysis is based on 40-80 km wide segments that average out along strike changes in the large-scale structure. Therefore the characteristic present-day large-scale structure is not significantly different from the structure displaced by 30 km.

Conclusions

The major conclusions of this study are as follows:

1. The large-scale topography across DSR, between Lake Kinneret and the Gulf of Elat, shows a distinct asymmetrical pattern across the rift: the eastern side topography is higher and its overall shape resembles an uplifted shoulder; the western side resembles a wide arch.

2. Along-strike variations of the topography are characterized by five segments that differ from one another by the shape and height of the uplifted shoulder on the eastern side and by the amplitude and wavelength of the arch on the western side.

3. Elevation variations along the rift axis show a parallel trend with the highest points on the eastern side of the rift and a mirror image trend with the highest points on the western side.

4. The large-scale structure across the rift (100-200 km wide) also shows an asymmetrical pattern, similar to that of the topography asymmetry. The rift's eastern margin is uplifted toward the rift margin, whereas the rift's western margin is downflexed toward the rift axis, and its overall shape resembles an asymmetrical monocline (arching).

5. The large-scale topographic and structural asymmetries reflect a wide half-graben structure (30-60 km wide), in which the boundary fault lies along the rift eastern margin and is inclined westward. The hanging wall, along the rift's western side, is tilted from its hinge along the Judea/Negev mountain belt eastward to the rift axis.

6. The transtensional tectonic environment along the DSR shows a scale dependent deformation partitioning: regional scale structure indicates vertical motion along the rift, whereas narrower scale structures, which are representative of the horizontal motion, are observed within the rift valley.

7. The morphology and the structure of the rift's eastern margin reflect a broad regional uplift along the DSR. The topography and structure of the rift's western

side lack the characteristic features of an uplifted rift margin because it comprises the hanging wall of a wide half-graben structure.

8. The western side arching, which formed partly contemporaneously with the formation of the rift in the Pliocene, cannot be explained as a compressional structure of neither the SAS or DSS stress fields. We explain its formation as a subsidary structure of the main rift structure, in which the western slope of the arching reflects the initially inclined prerift topography, and the eastern slope reflects the downward flexure of the rift's western margin toward the rift axis.

Appendix: Stratigraphic Considerations

The stratigraphic units which are used in the present study are the same as those mapped on the 1:750,000 scale photomap produced by *Bartov* [1990]. The stratigraphic units' nomenclature and thickness are provided in Table 1. Here we present a brief description of these units.

Paleozoic: The Nubian Sandstone (NS)

This rock unit includes all Paleozoic rocks from the Cambrian to the lower Permian. Relicts of the Paleozoic sequence show a regional deposition of mainly continental sandstone with shallow marine intercalations [*Weissbrod*, 1981]. Two major erosional events, which occurred in the Carboniferous and in the Early Cretaceous, removed most of the sequence in the southern parts of the studied area [*Bender*, 1968, 1974; *Weissbrod*, 1981].

Late Paleozoic - Early Mesozoic (PM)

This stratigraphic unit contains mainly Early Mesozoic (Triassic-Jurassic) rock units and some late Paleozoic (upper Permian) units in the subsurface. The PM unit is bounded between two major unconformities: the Late Carboniferous (at the base) and the Early Cretaceous (at the top). This unit contains shallow marine sediments intercalating with continental sandstone [*Drukman*, 1974; *Goldberg and Friedman*, 1970; *Garfunkel*, 1978]. These intercalations represent a regional facies transition from shallow marine at a distance of 50-100 km from the present-day coast to mainly continental 100-200 km farther inland. The Early Cretaceous erosional events differentially removed a major part of this unit in the southern Negev and southern Jordan (south of the Dead Sea) [*Garfunkel*, 1988]. As a result, this unit cannot serve as a regional stratigraphic marker.

Early Cretaceous (LC)

The Early Cretaceous rocks occur throughout the entire studied area, exposed in a few eroded fold structures, mainly along the Judean and the Negev Mountains. Throughout most of the studied area the unit consists of continental sandstone interbedded with a few marine carbonates [*Garfunkel*, 1978]. The ratio of carbonate to sandstone increases to the northwest together with the increase of thickness (up to 1100 m under the coastal plain [*Cohan*, 1971]). In southern Israel and central Jordan, these rocks overlie unconformably the PM and the NS rock units and, farther south, even the crystalline basement [*Garfunkel*, 1978]. The regional distribution of the Early Cretaceous sediments, combined with the underlying erosional surface, provides a reliable stratigraphic marker.

Cretaceous and Early Tertiary (K_j, K_s, and T_a)

A slow subsidence of the area accompanied by global sea level rise, which lasted from the Early Cretaceous to the late Eocene, established a shallow water carbonate platform over much of Israel [*Garfunkel*, 1978]. The carbonitic-rich sequence deposited by this transgression is subdivided into three units: the Cenomanian-Turonian Judea Group (K_j), the Senonian-Paleocene Mount Scopus Group (K_s), and the Eocene Avedat Group (T_a).

The Judea Group was deposited during the first stage of the Late Cretaceous transgression, which penetrated inland 200-300 km from the present-day coast line (all the way to southern Sinai). The carbonates of the Judea Group are widely exposed throughout the studied area. This carbonate cover is characterized by relatively uniform, slowly changing facies, indicating deposition on a stable platform [*Bartov*, 1974; *Bartov and Steinitz*, 1977; *Garfunkel*, 1978]. Therefore this extensively exposed rock unit is the best stratigraphic marker in the region.

The Mount Scopus Group contains chalk, chert, and marl that were deposited during the Senonian and the Paleocene. This soft rock unit unconformably overlies the hard carbonates of the Judea Group. This transition between the rock units is associated with a major change in the marine environments, resulting in a replacement of the shallow marine carbonates by pelagic chalk of a deeper marine environment [*Picard*, 1951; *Bentor and Vroman*, 1951, 1960]. Facies and thickness variations within this rock unit indicate synsedimentation growth of the Syrian Arc Fold Belt (SAFB), which extends from Syria through Israel to northern Sinai [*Garfunkel*, 1978]. The thickness differences between the deepest syncline and the adjacent anticlines (5-30 km horizontal distance) can reach several hundred meters. These thickness changes raise difficulties in using the Mount Scopus Group rock units as reliable stratigraphic markers.

The Avedat Group is comprised mostly of chalks and limestones of Eocene age. This rock unit was deposited

during the last stage of the late Mesozoic transgression that penetrated more than 1000 km south of the present coast line. Facies and thickness variations within this rock unit indicate the continuous growth of the SAFB in the Eocene but at a slower rate. Rapid sedimentation and declining tectonic activity resulted in gradual covering of the SAFB structural relief by marine sediments [*Avni*, 1989]. Thus the Top Eocene Sequence formed a flat sedimentary surface, gently inclined toward the open sea in the northwest. This Top Eocene is the youngest isochronous morphosedimentary marker that has a regional distribution and thus can be used to detect post-Eocene tectonic deformation.

Neogene - Quaternary (NQ)

This rock unit consists of continental sediments and is subdivided into prerift and postrift sedimentary sequences. The Miocene prerift sequence consists mainly of fluvial-lacustrine sediments in the east and shallow marine carbonates west of the SAFB. The continental facies (Hazeva Formation [*Bentor and Vroman*, 1957]) contains mainly sandstone with clay lenses and few lacustrine limestone interbeds. The clasts in the unit were derived mainly from areas located southeast of the DSR [*Bentor and Vroman*, 1960; *Garfunkel and Horowitz*, 1966] and transported northwestwardly by a regional fluvial system, which drained to the Mediterranean. Because of young erosion, the thickness of the Miocene sequence varies from 0 to 1000 m (in the Karkom graben [*Bartov and Garfunkel*, 1980]), or may be up to 2000 m, as found recently in the northern Arava Valley (Bartov, personal communication, 1994).

The postrift sediment sequence consists of fluvial-lacustrine sediments which were accumulated within the rift. The development of the rift as a deep, inland erosional base level triggered a major change in the regional fluvial system that prevailed in the study area. While sedimentation was confined to the rift and to parts of its newly forming drainage systems, most of the elevated areas on both sides of the rift were undergoing intensive erosion. The sedimentary character of the postrift rock units was highly influenced by the nature of the drainage basin from which they were derived and by the local environments in the depositional basin (stream, alluvial fan, playa, or lake). Therefore they consist of diverse fluvial facies, fresh and saline lacustrine sediments, and few marine intercalations.

Acknowledgments. We are thankful to Michael Steckler, Cindy Ebinger, Jan-Diederik Van Wees, and an anonymous reviewer for very helpful comments. We would also like to thank Amotz Agnon, Gidi Baer, Ariel Haiman, Ze'ev Reches, and Jilles Wust for useful discussions and comments. We are grateful to John K. Hall for providing topographic profiles from the Digital Terrain Model (DTM) of Israel and adjacent areas. This DTM, on a 25 m grid with decimeter resolution, was prepared at the Geological Survey of Israel from 1:50,000 scale topographic maps and is copyrighted property of the Survey of Israel. The DTM includes extensive data on adjacent marine and land areas. This study was supported by the Minerva Dead Sea Research Center at Tel Aviv University.

References

Avni, Y., The geology, paleogeography and evolution of landscape in the central Negev and the western Ramon structure (in Hebrew, English abstract), M.Sc. thesis, 153 pp., Hebrew Univ., Jerusalem, 1989.

Ball, M.W., and D. Ball, Oil prospects of Israel, *Am. Assoc. Pet. Geol. Bull., 37*, 1-113, 1953.

Bartov, Y., A structural and paleogeographic study of the Central Sinai faults and domes (in Hebrew, English abstract), Ph.D. thesis, 143 pp., Hebrew Univ., Jerusalem, 1974.

Bartov, Y., Geological photomap of Israel and adjacent areas, scale 1:750.000, Isr. Geol. Surv., Jerusalem, 1990.

Bartov, Y., and Z. Garfunkel, Relations between clastic sediments and tectonic history of the Karkom graben, paper presented at Annual Meeting, *Israel Geol. Soc.*, 1980.

Bartov, Y., and G. Steinitz, The Judea and the Mount Scopus groups in the Negev and Sinai with trend surface analysis of thickness data, *Isr. J. Earth Sci., 26*, 119-148, 1977.

Bartov, Y., Y. Eyal, Z. Garfunkel, and G. Steinitz, Late Cretaceous and tertiary stratigraphy and paleogeography of southern Israel, *Isr. J. Earth Sci., 21*, 69-97, 1972.

Ben Avraham, Z., and U. ten Brink, Tranverse faults and segmentation of basins within the Dead Sea Rift, *J. Afr. Earth Sci., 8*, 603-616, 1989.

Bender, F., *Geologie von Jordanien*, pp. 1-230, Gerbruder Borntraeger, Berlin, 1968.

Bender, F., Explanatory note on the geological map of Wadi Araba, Jordan, *Geol. Jahrb. Reihe B, 10*, 3-62, 1974.

Bentor, Y., and A. Vroman, The geological map of the Negev, sheet 18, Abde (Avedat)(in Hebrew), 1st ed., scale 1:100,000, pp. 1-98, Isr. Geol. Surv., Jerusalem, 1951.

Bentor, Y., and A. Vroman, A structural contours map of Israel (1:250.000) with remarks on its dynamic interpretation, *Bull. Geol. Surv. Isr., 7*, 1-10, 1954.

Bentor, Y., and A. Vroman, The geological map of the Negev, sheet 19, Arava Valley, with explanatory notes, scale 1:100,000, pp. 1-66, Isr. Geol. Surv., Jerusalem, 1957.

Bentor, Y., and A. Vroman, The geological map of the Negev, sheet 16, Mt. Sedom, with explanatory text (rev. ed.), scale 1:100,000, pp. 1-117, Isr. Geol. Surv., Jerusalem, 1960.

Bentor, Y., and A. Vroman, The geological map of the Negev, sheet 20, Mt. Lotz, scale 1:100,000, pp. 1-62, Isr. Geol. Surv., Jerusalem, 1964.

Blanckenhorn, M., *Die strukturlinien des Rotes Meeres*, pp. 115-180, *Richthofen-Festschr*, Berlin, 1893.

Cohan, Z., The geology of the Lower Cretaceous of the Helez field, Israel (in Hebrew, English abstract), Ph.D thesis, 98 pp., Hebrew Univ., Jerusalem, 1971.

Druckman, Y., The stratigraphy of the Triassic sequence in southern Israel, *Bull. Geol. Surv. Isr., 64*, 1-92, 1974.

Ebinger, C.J., T.D. Bechtel, D.W. Forsyth, and C.O. Bowin Effective elastic plate thickness beneath the East African and Afar Plateaus and dynamic compensation of the uplift, *J. Geophy. Res., 94*, 2883-2901, 1989.

El-Isa, Z., J. Mechie, C. Prodehl, J. Makris, and R. Rihmn, A crustal structure study of Jordan derived from seismic refraction data, *Tectonophysics, 138*, 235-253, 1987.

Eyal, Y., Stress field fluctuations along the Dead Sea rift since the middle Micene, *Tectonics, 15*, 157-170, 1996.

Eyal, Y., and A. Negev. The deformation history of the Givat Hayil area (northern Negev, Israel) based on mesostructures, *Isr. J. Earth Sci., 40*, 151-160, 1991.

Eyal, Y. and Z. Reches, Tectonic analysis of the Dead Sea Rift region since the Late Cretaceous, based on mesostructures, *Tectonics, 2*, 167-185, 1983.

Freund, R., Z. Garfunkel, I. Zak, M. Goldberg, T. Weissbrod, and B. Derin, The shear along the Dead Sea Rift, *Philos. Trans., R. Soc. London., ser. A, 267*, 107-130, 1970.

Garfunkel, Z., The Negev–regional synthesis of sedimentary basins, paper presented at 10th International Congress on Sedimentology, Jerusalem, 1978.

Garfunkel, Z., Internal structure of the Dead Sea leaky transform (rift) in relation to plate kinematics, *Tectonophysics, 80*, 81-108, 1981.

Garfunkel, Z., Relations between continental rifting and uplifting: Evidence from the Suez rift and northern Red Sea, *Tectonophysics, 150*, 33-49, 1988.

Garfunkel, Z. and A. Horowitz, The upper Tertiary and the Quaternary morphology of the Negev, *Isr. J. Earth Sci., 15*, 101-117, 1966.

Ginzburg, A., and Y. Folkman, The crustal structure between the Dead Sea Rift and the Mediterranean Sea, *Earth Plant. Sci. Lett., 51*, 181-188, 1980.

Ginzburg, A., and Y. Folkman, Geophysical investigation of crystalline basement between Dead Sea Rift and Mediterranean Sea, *Am. Assoc. Pet. Geol. Bull., 65*, 490-500, 1981.

Goldberg, M., and G.M. Friedman, Paleoenvironments and paleogeographic evolution of the Jurrasic system in southern Israel, *Bull. Geol. Surv. Isr., 61*, 1-44, 1970.

Gvirtzman, G., The Saqiye Group (Late Eocene - Early Pleistocene) in the Hashfela and Coastal Plain of Israel (in Hebrew, English abstract), *Isr. Geol. Surv. Rep., Od/5/6*, 1-170, 1970.

Hall, J.K., The GSI terrain model (DTM) project completed, *Isr. Geol. Surv. Curr. Res., 8*, 47-50, 1993.

Haq, B.U., J. Hardenbol, and, P.R. Vail Chronology of fluctuating sea levels since the Triassic, *Science, 162*, 1156-1166, 1987.

Joffe, S., and Z. Garfunkel, Plate kinematics of the circum Red Sea - A reevaluation, *Tectonophysics, 141*, 5-22, 1987.

Kovach, R.L., and Z. Ben Avraham, Gravity anomalies across the Dead Sea rift and comparison with other rift zones, *Tectonophysics, 111*, 155-162, 1985.

Lartet, M.L., Essai sur la geologie de la Palestine et des contrees avoisinantes, *Ann. Sci. Geol., 1*, 5-116, 1869.

Masek, J.G., B.L. Isacks, and E.J. Fielding, Rift flank uplift in Tibet: Evidence for a viscous lower crust, *Tectonics, 13*, 659-667, 1994a.

Masek, J.G., B.L. Isacks, T.L. Gubbels, and E.J. Fielding, Erosion and tectonics at margins of continental plateaus, *J. Geophy. Res., 99*, 13,941-13,956, 1994b.

Mimran, Y., Unconformities on the eastern flank of the Fari'a Anticline and their implications on the structural evolution of Samaria (central Israel), *Isr. J. Earth Sci., 33*, 1-11, 1984.

National Geophysical Data Center (NGDC), ETOPO-5 bathymetry-topography data NOAA, report U.S. Dep. of Commer., Boulder, Colo., 1988.

Picard, L., Structure and evolution of Palestine, Bulletin, pp. 1-187, Geol. Dep. Hebrew Univ., Jerusalem, 1943.

Picard, L., Geomorphogeny of Israel, 1, The Negev, *Isr. Res. Counc. Bull., 8G*, 1-30, 1951.

Picard, L., Geological cross-sections, in *Atlas of Israel*, Sheet 2/III, Surv. of Israel, Jerusalem, 1960.

Picard, L., Thoughts on the graben systems of the Near East, *Pap. Geol. Surv. Can., 66(14)*, 22-34, 1966.

Picard, L., The Elat (Aqaba) - Dead Sea - Jordan subgraben system, *Tectonophysics, 141*, 23-32, 1987.

Powell, J.H., Stratigraphy and sedimentation of the Phanerozoic rocks of central and south Jordan, B, Kurnub, Ajlun and Belqa groups, *Geol. Mapp. Div. Bull. 11B*, Geol. Dir., Natural Resources Authority, Amman, Jordan, 1989.

Quenell, A. M., The structural and geomorphic evolution of the Dead Sea Rift, *Q. J. Geol. Soc. London, CXIV(1)*, 1-24, 1958.

Quenell, A.M., Tectonics of the Dead Sea Rift, paper presented at 20th International Geological Congress, Mexico, 1959.

Quenell, A.M., The western Arabia rift system, in *The Geological Evolution of the Eastern Mediterranean, Geol. Soc. Spec. Publ., 17*, 775-787, 1984.

Rosendahl, B.R., Architecture of continental rift with special reference to East Africa, *Annu. Rev. Earth Planet. Sci., 15*, 445-503, 1987.

Salamon, A., The monoclines in the northern Negev: A model of tilted blocks and shortening (in Hebrew, English abstract), pp. 101, M.Sc. thesis, Hebrew Univ., Jerusalem, 1-101, 1987.

Steckler, S.S., and G.I. Omar, Controls on erosional retreat of the uplifted rift flanks at the Gulf of Suez and northern Red Sea, *J. Geophy. Res., 99*, 12,159-12,173, 1994.

Steinitz, G. and Y. Bartov, The Miocene-Pleistocene history of the Dead Sea segment of the rift in light of K-Ar ages of basalts, *Isr. J. Earth. Sci., 40*, 199-208, 1991.

ten Brink U.S., N. Schoenberg, R.L. Kovach, and Z. Ben-Avraham, Uplift and possible Moho offset across the Dead Sea transform, in *Geologic and Tectonic Processes of the Dead Sea Rift Zone, Tectonophysics, 180*, 71-85, 1990.

ten Brink, U., Z. Ben Avraham, R.E. Bell, M. Hassouneh, D.F. Coleman, G. Andreasen, G. Tibor, and B. Coakley, Structure of the Dead Sea pull-apart basin from gravity analyses, *J. Geophy. Res., 98*, 21,877-21,894, 1993.

Wdowinski, S., and Y. Bock, The evolution of deformation and topography of high elevated plateaus, 2, Application to the Central Andes, *J. Geophys. Res., 99*, 7121-7130, 1994.

Wdowinski, S., and R. J. O'Connell, On the choice of boundary conditions in continuum models of continental deformation, *Geophys. Res. Lett., 17*, 2413-2416, 1990.

Wdowinski, S., and E. Zilberman, Kinematic modeling of large-scale rift-related structural asymmetry across the Dead Sea Rift, in *Dynamics of extensional basins and inversion tectonics, Tectonophysics, 266*, 187-201, 1996.

Weissbrod, T., The Paleozoic of Israel and adjacent countries (lithostratigraphic study), *Rep. Mp/600/81*, pp. 1-276, Isr. Geol. Surv., Jerusalem, 1981.

Wetzel, R., and D.M. Morton, Contribution a la geologie la Trans Jordanie, *Notes Mem. Moyen Orient, 7*, 95-141, 1959.

Wilson, J. T., A new class of faults and their bearing on continental drift, *Nature, 207*, 343-347, 1965.

Zilberman, E., The Tertiary and the Quaternary of the northwestern Negev, in Outlines of the geology of the northwestern Negev, edited by Z.B. Begin, *Rep. GSI/19/84*, pp. 41-76, Isr. Geol. Surv., Jerusalem, 1984.

Zilberman, E., Landscape evolution in the central, northern and northwestern Negev during the Neogene and the Quaternary, *Rep. GSI/45/90*, pp. 1-108, Isr. Geol. Surv., Jerusalem, 1990.

Zilberman, E., Remnants of Miocene landscape in the central and northern Negev and their paleogeographic implications, *Bull. Geol. Surv. Isr., 83*, 1-54, 1992.

S.Wdowinski, Department of Geophysics and Planetary Sciences, Tel Aviv University, Ramat Aviv, 69978, Israel. (e-mail: shimon@geo1.tau.ac.il)

E. Zilberman, Geological Survey of Israel, 30 Malkhe Israel St., Jerusalem, Israel. (e-mail: zilberman@post.gsi.gov.il)

(Received May 13, 1996;
revised November 18, 1996;
accepted January 24, 1997.)